Supplementary data

Enhanced electromagnon excitations in Nd-doped $BiFeO_3$ nanoparticles near morphotropic phase boundaries

Yuan Zhang,[1]† Yi Zhang,[1]† Quan Guo,[2] Dongwen Zhang,[2] Shuaizhi Zheng,[1] Ming Feng,[3] Xiangli Zhong,[1*] Congbing Tan,[1] Zhihui Lu,[2] Jinbin Wang,[1] Pengfei Hou,[1] Yichun Zhou[1] and Jianmin Yuan[2*]

[1]School of Materials Science and Engineering, Xiangtan University, Hunan 411105, China;

[2]Department of Physics, College of Science, National University of Defense Technology, Hunan 410073, China;

[3]Key Laboratory of Functional Materials Physics and Chemistry of the Ministry of Education, Jilin Normal University, Changchun 130103, China

---

† These authors contributed equally to this work.

* Authors to whom the correspondence should be addressed: e-mail: xlzhong@xtu.edu.cn

* Authors to whom the correspondence should be addressed: e-mail: jmyuan@nudt.edu.cn

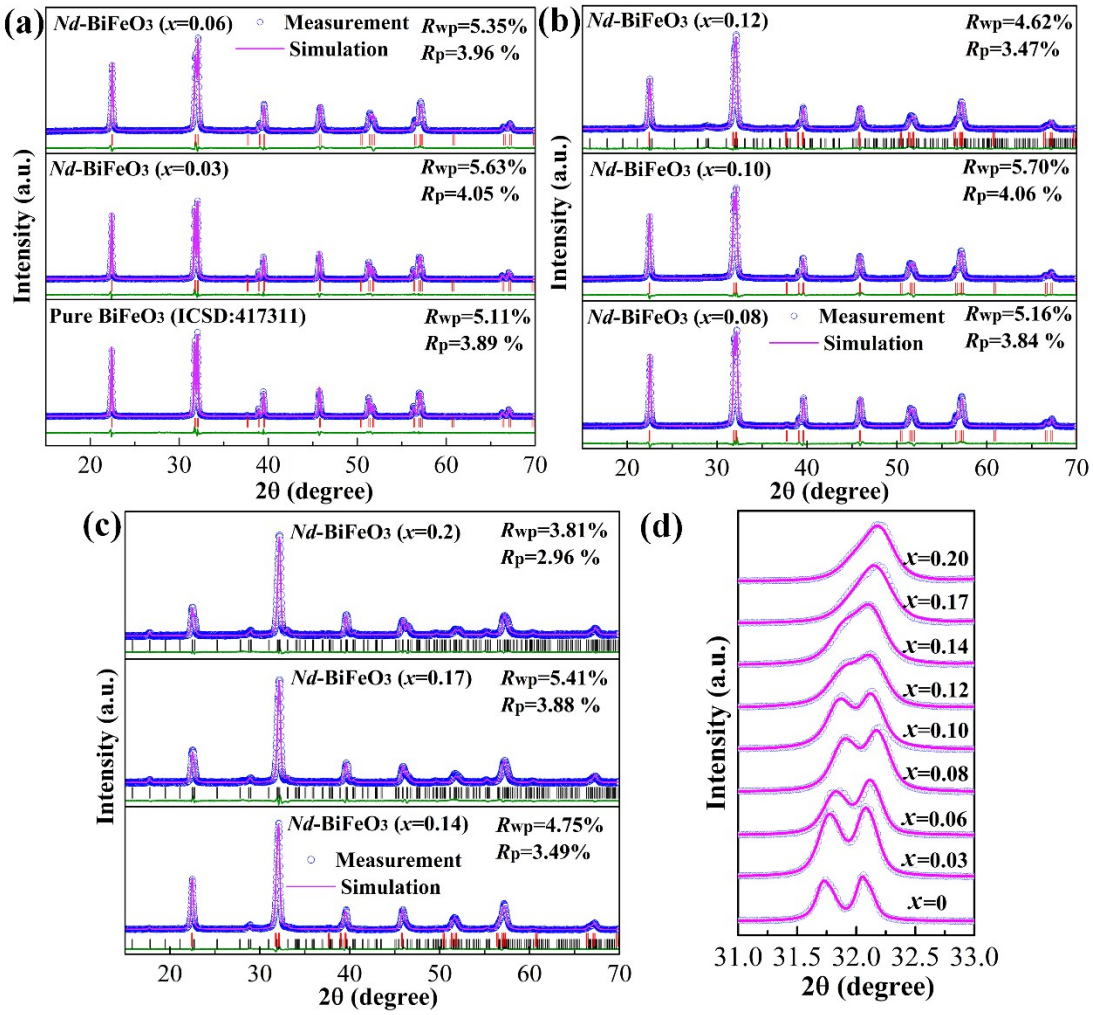

Figure S1 (a-c) Comparison between the measured and simulated XRD patterns for $Bi_{1-x}Nd_xFeO_3$ ($BNFO_x$) nanoparticals in the range of x=0~0.2. (d) The magnified patterns of (104) and (110) diffraction peaks.

The Rietveld refined XRD patterns of $Bi_{1-x}Nd_xFeO_3$ samples are shown in details in Figure S1 respectively, it can be found that the simulated XRD results are coincide well with the measured results and the lattice parameters can be defined.

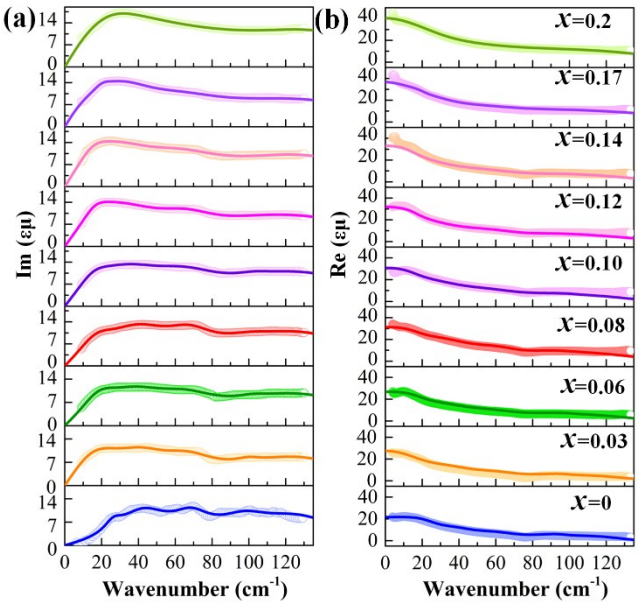

Figure S2 THz spectra of (a) imaginary ($\varepsilon\mu$), and (b) real parts ($\varepsilon\mu$) of $BNFO_x$ nanoparticles.

As the pellets for THz spectra were prepared by mixing $Bi_{1-x}Nd_xFeO_3$ ($BNFO_x$) nanoparticles with pure polyethylene (PE) power, the complex dielectric is characterized by effective medium theories of Polder and van Santen models for rods $\frac{\varepsilon_R-\varepsilon_h}{5\varepsilon_R+\varepsilon_p}=f_p\frac{\varepsilon_p-\varepsilon_h}{3(\varepsilon_p+\varepsilon_R)}$ to eliminate the influence of the mixed PE power.[1] The ε_p, ε_h and ε_R are the permittivity of the $BNFO_x$ nanoparticles, host pure PE power and mixtures, respectively. The f_p is the volumetric particle fraction ($0<f_p<1$) of the doping $BNFO_x$ nanoparticles with the relation of $f_p=f_w/(f_w+(1-f_w)\rho_p/\rho_h)$, and the f_w is the weight fraction of $BNFO_x$ nanoparticles and pure PE. The ρ_p and ρ_h is the densities of $BNFO_x$ nanoparticles and pure PE power, respectively.[2-6] The fitted parameters are shown in Table *SI* with the high-frequency permittivity of ε_∞=4.0 in all nanoparticles.

Table *SI* Fitted parameters of electomagnons modes *1* and *2*, and, phonon modes E_1, E_2 and A_1 for the $BNFO_x$ nanoparticles with ε_∞=4.0 .[7]

Mode	x	0	0.03	0.06	0.08	0.10	0.12	0.14	0.17	0.20
EM	γ_1(cm^{-1})	11.97	40.04	26.47	24.81	25.88	17.29	26.92	9.53	…
	γ_2(cm^{-1})	36.28	39.60	50.75	46.24	55.45	71.87	55.65	51.06	44.92
PH	$\Delta\varepsilon_1$	2.22	2.92	2.88	2.28	2.22	0.68	4.67	5.13	18.81
	γ_1(cm^{-1})	26.69	40.41	44.51	34.01	43.68	23.86	59.32	331.33	315.9
	$\Delta\varepsilon_2$	1.69	0.23	0.19	2.22	1.81	5.95	0.96	11.39	3.03
	γ_2(cm^{-1})	35.19	18.05	21.47	88.02	131.77	258.6	111.17	208.22	79.16
	$\Delta\varepsilon_3$	3.48	4.54	5.76	5.39	6.5	4.14	6.92	1.70	6.27
	γ_3(cm^{-1})	61.97	81.05	94.08	88.5	103.76	97.48	105.1	66.96	239.7

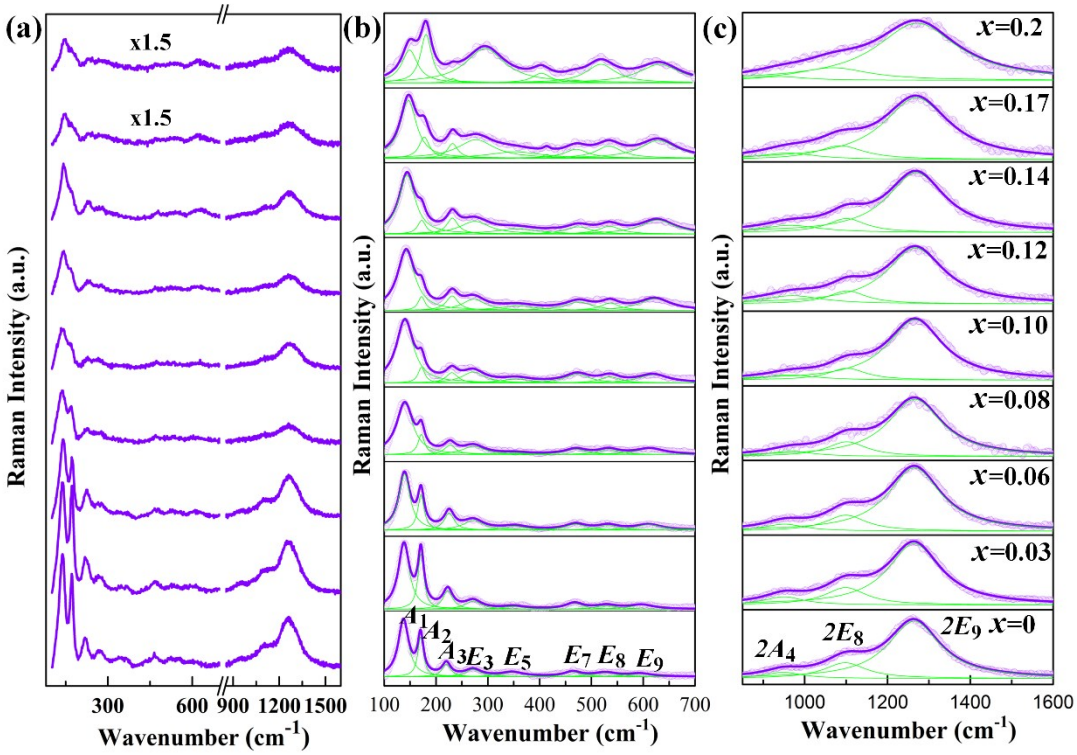

Figure S3 (a) Measured un-polarized Raman spectra for $BNFO_x$ nanoparticles between 100~1600 cm^{-1}. (b) A magnified view between 100~700 cm^{-1} fitted by Lorentzian function. (c) A magnified view between 850~1600 cm^{-1} fitted by Lorentzian function.

In the *R*3*c* BFO structure, the ferroelectric distortion originates from the stereochemical activity of Bi^{3+} $6s^2$ lone electron pair, where the Fe-O-Fe bond angle gives strong antiferromagnetic superexchange interaction.[8, 9] The Bi atoms only participate in low-frequency modes up to 167 cm^{-1}, while the Fe atoms are mainly involved in modes between 152~262 cm^{-1} with possible contributions to some higher-frequency modes, and the motion oxygen atoms dominate the modes above 262 cm^{-1}.[9] The higher frequency orders of *E* modes at 900~1600 cm^{-1} may be associated with the strong coupling of spin-lattice from the interaction of adjacent magnetic sub lattices of BFO,[10] since they are related to the octahedral rotation with critical role of weak magnetism. Obviously, the A_1 and low frequency *E* modes (<400 cm^{-1}) play an important role in ferroelectrics, which all mainly contributes to Bi-O bonds, while the $2E_8$ and $2E_9$ modes exhibit essential roles in antiferromagnetism through superexchange. Therefore, the un-polarized Raman scattering spectra of $BNFO_x$ nanoparticles at 0~1600 cm^{-1} are measured at room temperatures shown in Figure S3(a). Three sharp peaks below 250 cm^{-1} are assigned as A_1, A_2 and A_3 modes, and the three peaks at high frequency of 900~1600 cm^{-1} are labeled $2A_4$, $2E_8$ and $2E_9$ modes. One can see that these six peaks are weaken in intensities and broaden in linewidth gradually. The measured spectra are fitted by decomposing the curves into individual Lorentzian components shown in Figure S3(b) and S3(c), where the peak positions of each component are obtained.

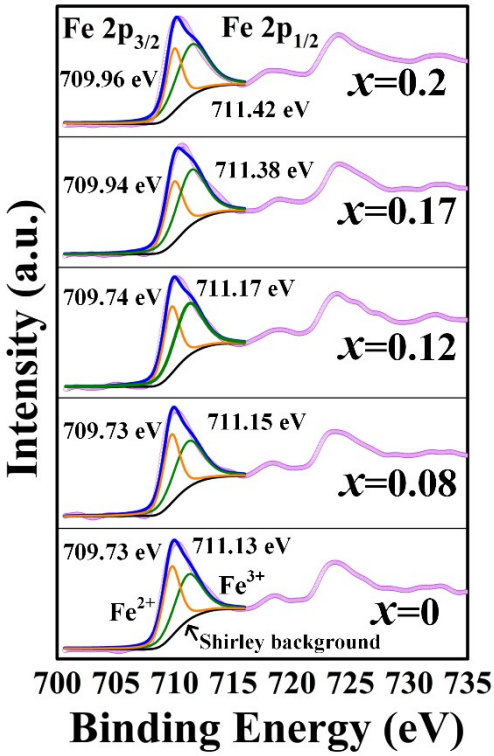

Figure S4 Fe 2p XPS spectra of $BNFO_x$ nanoparticles.

The Fe 2*p* spectra are shown in Figure S4 with the C 1s peak at 286.58 eV. It can be found that the Fe 2*p* core level consists of two components of $2p_{3/2}$ (710.43 eV) and $2p_{1/2}$ (724.01 eV) with spin-orbit splitting energy of 13.58 eV, which is coincident with the theoretical value of $\Delta_{Fe\ 2p}$ (13.6 eV) for Fe_2O_3.[11] When we fit the Fe $2p_{3/2}$ by mixed Gauss-Lorentz function of Shirley background, we can see that the binding energy of Fe $2p_{3/2}$ is composed of Fe^{2+} and Fe^{3+} at 709.73 eV and 711.12 eV in pure BFO, respectively. While the binding energy of Fe $2p_{3/2}$ at x=0.2 presents 709.96 eV for Fe^{2+} and 711.42 eV for Fe^{3+}, respectively. Obviously, the peaks of Fe $2p_{3/2}$ gradual shift into higher binding energy, which indicates an increasing bond strength between atoms.

REFERENCES:

(1). Scheller, M.; Jansen, C.; Koch, M. Applications of effective medium theories in the terahertz regime. *Recent Optical and Photonic Technologies*, *InTech*, 2010.

(2). Ung, B.; Dupuis, A.; Stoeffler, K.; Dubois, C.; Skorobogatiy, M. High-refractive-index composite materials for terahertz waveguides: trade-off between index contrast and absorption loss. *J. Opt. Soc. Am. B* **2011**, *28*, 917.

(3). Goian, V.; Kamba, S.; Kadlec, C.; Nuzhnyy, D.; Kužel, P.; Moreira, J. A.; Almeida, A.; Tavares, P. B. THz and infrared studies of multiferroic hexagonal $Y_{1-x}Eu_xMnO_3$ (x= 0-0.2) ceramics. *Phase Transit.* **2010**, *83*, 931.

(4). Sushkov, A. B.; Aguilar, R. V.; Park, S.; Cheong, S. W.; Drew, H. D. Electromagnons in Multiferroic YMn_2O_5 and $TbMn_2O_5$. *Phys. Rev. Lett.* **2007**, *98*, 027202.

(5). Aguilar, R. V.; Sushkov, A. B.; Zhang, C. L.; Choi, Y. J.; Cheong, S. W.; Drew, H. D. Colossal magnon-phonon coupling in multiferroic $Eu_{0.75}Y_{0.25}MnO_3$. *Phys. Rev. B* **2007**, *76*, 060404.

(6). Komandin, G. A.; Torgashev, V. I.; Volkov, A. A.; Porodinkov, O. E.; Spektor, I. E.; Bush, A. A. Optical Properties of $BiFeO_3$ Ceramics in the Frequency Range 0.3-30.0 THz. *Phys. Solid State* **2010**, *52*, 734.

(7). Kamba, S.; Nuzhnyy, D.; Savinov, M.; Šebek, J.; Petzelt, J.; Prokleška, J.; Haumont, R.; Kreisel, J. Infrared and terahertz studies of polar phonons and magnetodielectric effect in multiferroic $BiFeO_3$ ceramics. *Phys. Rev. B* **2007**, *75*, 024403.

(8). Yuan, G. L. Or, S. W.; Chan, H. L. W. Raman scattering spectra and ferroelectric properties of $Bi_{1-x}Nd_xFeO_3$ (x=0-0.2) multiferroic ceramics. *J. Appl. Phys.* **2007**, *101*, 064101.

(9). Hermet, P.; Goffinet, M.; Kreisel, J.; Ghosez, P. Raman and infrared spectra of multiferroic bismuth ferrite from first principles. *Phys. Rev. B* **2007**, *75*, 220102.

(10). Ramirez, M. O.; Krishnamurthi, M.; Denev, S.; Kumar, A.; Yang, S.-Y.; Chu, Y.-H.; Saiz, E.; Seidel, J.; Pyatakov, A. P.; Bush, A.; Viehland, D.; Orenstein, J.; Ramesh, R.; Gopalan, V. Two-phonon coupling to the antiferromagnetic phase transition in multiferroic $BiFeO_3$. *Appl. Phys. Lett*. **2008**, *92*, 022511.

(11). Huang, F.; Lu, X.; Lin, W.; Wu, X.; Kan, Y.; Zhu, J. Effect of Nd dopant on magnetic and electric properties of $BiFeO_3$ thin films prepared by metal organic deposition method. *Appl.*

Phys. Lett. **2006**, *89*, 242914.